PAPER

Check for updates

A SARS-Cov-2 sensor based on upconversion nanoparticles and graphene oxide†

Konstantina Alexaki, [ID] [a] Maria Eleni Kyriazi, [ID] [b] Joshua Greening, [a] Lapatrada Taemaitree, [c] Afaf H. El-Sagheer, [ID] [cd] Tom Brown, [ID] [c] Xunli Zhang, [ID] [ef] Otto L. Muskens [af] and Antonios G. Kanaras [ID] *[af]

Since the beginning of the COVID-19 pandemic, there has been an increased need for the development of novel diagnostic solutions that can accurately and rapidly detect SARS-CoV-2 infection. In this work, we demonstrate the targeting of viral oligonucleotide markers within minutes without the requirement of a polymerase chain reaction (PCR) amplification step *via* the use of oligonucleotide-coated upconversion nanoparticles (UCNPs) and graphene oxide (GO).

In 2019 a novel form of coronavirus was identified termed severe acute respiratory syndrome coronavirus 2. The disease, also known as COVID-19, was found to be highly transmissible amongst humans and in some cases fatal. This led to a global urgent requirement for the development of sensitive and specific diagnostic tools for the detection of the virus and its subsequent mutated versions.

The most reliable technique in clinical diagnosis relies on the detection of the RNA of SARS-CoV-2 using nucleic acid amplification technologies (NAATs) and primarily real-time polymerase chain reaction (RT-PCR).[1] This technique, although reliable, is hindered by the need for specialized equipment and long turnaround times. To address these limitations alternative diagnostic tools have recently been developed based on the use of biosensors. A biosensor platform typically consists of three important features, a bio-receptor such as a protein, a transducer component, and an amplification element. Most commonly the bio-receptor interacts with the biomarker of interest and induces a change, which depending on the transducer could be observed as an electrochemical, optical, electrical, or thermal change thus signalling the presence of the target.[2–4] These sensors represent a testing method that is sensitive and thus have recently been used for the detection of SARS-CoV-2 virus markers in order to control and diagnose COVID 19.[2,5] For example, Seo and co-workers reported the development of a field-effect transistor (FET) based biosensor for the detection of the SARS-CoV-2 spike protein. Their device was found to be highly sensitive towards the target and exhibited no cross-reactivity with the MERS-CoV-2 virus.[6] Furthermore, Lin *et al.* demonstrated a rapid and sensitive lateral flow immunoassay (LFIA) which consisted of lanthanide-doped polystyrene nanoparticles for the detection of anti-SARS-CoV-2 IgG in human serum.[7] Moitra and co-workers focused on the detection of viral RNA and developed a colorimetric assay based on the use of gold nanoparticles (AuNPs) functionalized with thiol-modified antisense oligonucleotides (ASOs) specific to the N-gene of SARS-CoV-2. In the presence of the target RNA, selective AuNP agglomeration was observed as indicated by the change in the surface plasmon resonance (SPR) of the AuNPs. The phosphodiester bonds of the SARS-CoV-2 RNA (N gene) strand were subsequently cleaved following the addition of RNaseH leading to a visually detectable precipitate mediated by the additional agglomeration of AuNPs. By testing against alternative RNA targets they confirmed not only the sensitivity but also the specificity of their method.[8] Fluorescence based detection was shown by Wang *et al.* who developed an immunoassay, implemented on a lateral flow strip for the detection of SARS-CoV-2 RNA. They made use of S9.6 monoclonal antibody-labelled europium-chelate-based fluorescent nanoparticles (FNP) capable of capturing double strands. Within 1 h they were able to detect the absence or presence of the RNA target *via* the use of a fluorescence analysis device with high sensitivity and specificity.[9]

When looking at the use of alternative sensors for the detection of COVID-19 there are some important objectives that

aSchool of Physics and Astronomy, Faculty of Engineering and Physical Sciences, University of Southampton, Southampton SO17 1BJ, UK. E-mail: a.kanaras@soton.ac.uk

bCollege of Engineering and Technology, American University of the Middle East, Kuwait

cDepartment of Chemistry, University of Oxford, Chemistry Research Laboratory, 12 Mansfield Road, Oxford OX1 3TA, UK

dChemistry Branch, Department of Science and Mathematics, Faculty of Petroleum and Mining Engineering, Suez University, Suez 43721, Egypt

eSchool of Engineering, Faculty of Engineering and Physical Sciences, University of Southampton, Southampton SO17 1BJ, UK

fInstitute for Life Sciences, University of Southampton, Southampton, SO171BJ, UK

should be taken into consideration. First the sensor should be highly selective and specific, which means that it should bind rapidly and accurately only to the target molecules. Second, the sensor must detect the target molecule to the smallest possible amounts to enable early diagnosis (*e.g.* important for controlling the spread of a disease). Third the sensor should be easy and cheap to fabricate in large scales so that it can be easily commercialized. Furthermore, it needs to be stable in a range of conditions (*e.g.* temperature variations during transportation) as well as being made by non-toxic materials to avoid contamination of the environment.

An interesting oligonucleotide sensor, which we have recently developed, and takes into consideration the aforementioned points, involves the use of UCNPs and GO. This sensor uses a co-doping system of $NaYF_4$:Yb^{3+}, Er^{3+} UCNPs, which comprises of three components: a host matrix ($NaYF_4$), sensitiser (Yb^{3+}) and activator (Er^{3+}).[10] One important advantage involving the use of UCNPs is the ability to easily modify their surface with synthetic oligonucleotides. In the presence of GO, 'π–π stacking' intermolecular interactions take place between the oligonucleotide aromatic bases and the sp^2 hybridised carbon structure of GO, leading to adsorption of the UCNPs on the GO surface and complete fluorescence quenching of the system.[11] Previous research has suggested that when UCNPs and GO are used as a donor/acceptor pair, a FRET quenching mechanism is adopted. The energy transfer is based on donor–acceptor dipole–dipole interactions and depends on the degree of overlap between absorption and emission spectra as well as the donor–acceptor distance, which should be less than 10 nm.[11–15] In the presence of the complementary oligonucleotide target, preferential hydrogen bond hybridisation of bases occurs and UCNPs can no longer adsorb to the GO surface. Fluorescence quenching therefore no longer occurs and a fluorescence signal is recorded.[16] We have previously shown how such a biosensor could successfully be used for the detection of Alzheimer's and prostate cancer mRNA markers in the presence of complex biological environments such as human blood serum and cell lysate.[17] We also demonstrated the construction of a portable sensor and its use in the field for the detection of mRNA biomarkers related to Zn deficiency in crops.[18]

In this paper, we demonstrate the construction of an UCNP/GO biosensor for the sensitive and rapid detection of oligonucleotide markers associated with the SARS-CoV-2 virus as shown in Scheme 1. UCNPs were functionalized with oligonucleotides designed to detect part of the viral genome coding for the RNA-dependent RNA polymerase (RdRp)/Helicase (Hel), a marker that is also used in RT-PCR testing.[19] We show that the presence of the target can be detected within a few minutes with excellent selectivity and sensitivity.

A solvothermal method was used for the synthesis of hexagonal phase β-$NaYF_4$:Yb^{3+} (20%), Er^{3+} (2%) upconversion nanoparticles (core UCNPs).[18,20] Fig. 1 shows the resulting core UCNPs, which were highly monodisperse with an average size of 33 ± 1 nm (Fig. 1A and C). Core UCNPs were further coated with an additional shell of $NaYF_4$, which has been proven to enhance the upconversion fluorescence emission as presented in Fig. S1.†[21] The shell was achieved by following a slightly
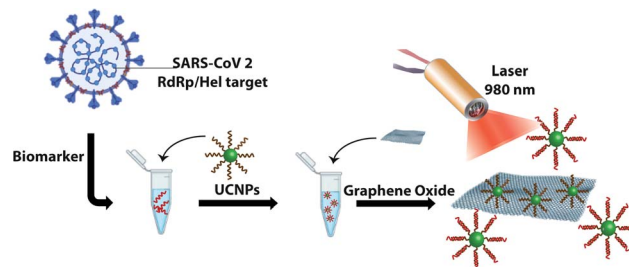
Scheme 1 Detection of an oligonucleotide target associated with the RdRp/Hel gene of SARS-CoV-2. Oligonucleotide-coated UCNPs designed to detect part of the SARS-CoV-2 gene are incubated with the target of interest. Upon addition of GO and irradiation with a laser at 980 nm, the fluorescence signature originating from the UCNPs is monitored. The absence of a fluorescence signal would indicate that the target is not present and fluorescence quenching has taken place following adsorption of the nanoparticles onto the GO surface.

modified version of a previously reported method.[18] The resulting core–shell UCNPs retained their uniform shape and had a larger average size of 37 ± 1 nm (Fig. 1B and D) due to the shell formation.

The synthesised nanoparticles demonstrated the expected fluorescence signal corresponding to ytterbium and erbium doped $NaYF_4$ nanoparticles following excitation with a 980 nm laser. The fluorescence spectrum demonstrated two distinct peaks at 540 nm and 655 nm (see Fig. S1†) where the green emission peak at 540 nm corresponded to the $^4S_{3/2} \rightarrow {}^4I_{15/2}$ transition and the red emission peak at 655 nm corresponded to the $^4F_{9/2} \rightarrow {}^4I_{15/2}$ transition.[22] Following their synthesis, UCNPs were well dispersed in hexane and a number of surface modification steps were subsequently followed in order to achieve water solubility and the covalent attachment of single-stranded DNA (ssDNA) sequences on the UCNP surface.

Following the successful multi-step synthesis and characterisation of single-stranded oligonucleotide coated UCNPs
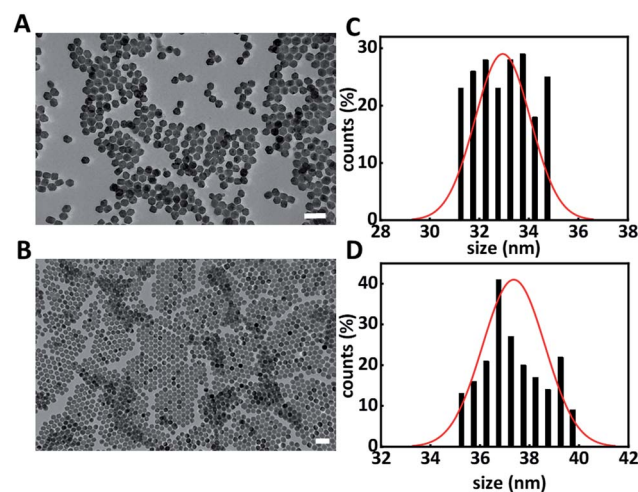

Fig. 1 Representative transmission electron microscopy images of core (A) and core–shell UCNPs (B) and their corresponding size distribution histograms (C and D). Scale bar is 100 nm.

(ssDNA-UCNPs), we evaluated the ability of GO to quench UCNP fluorescence by performing a calibration experiment. This was aimed to determine the optimum UCNP/GO ratio for complete UCNP fluorescence quenching. Fig. 2A shows that by gradually increasing the concentration of GO, whilst maintaining the same concentration of UCNPs (0.5 mg mL^{-1}) a steady decrease in the fluorescence intensity was observed with maximum quenching observed at a GO concentration of 0.6 mg mL^{-1}.

We further correlated the change in fluorescent intensity at λ_{max} for each UCNP peak upon the addition of GO. Fig. 2B shows the change in fluorescence intensity at wavelengths of 540 nm and 655 nm as a function of GO concentration. Upon the addition of 0.6 mg mL^{-1} of GO to the oligonucleotide coated UCNP solution, the fluorescence signal was almost completely quenched.

SARS-CoV-2 is a positive strand RNA virus with a genome that is approximately 30 kb in size. One core component of the virus genome is known as RNA dependant RNA polymerase (RdRp) and is critical for the replication and transcription of viral RNA.[23] Amongst other targets, the detection of RdRp *via* RT-PCR has been reported to have the highest analytical sensitivity and it was chosen as a target for our sensor.[19]

Following calibration experiments, we proceeded to determine whether our sensor could efficiently detect the presence of the RdRp target. In the absence of a target and upon incubation with GO (0.6 mg mL^{-1}), no fluorescence signal could be detected. For the target experiment, the ssDNA-UCNPs were hybridized to their complementary DNA (cDNA) (see Table S1†) and then GO was added. Fig. 3 presents the results obtained after hybridisation with an increasing concentration of cDNA target for 30 min. A decrease in the quenching efficiency of GO (Fig. 3A) over both characteristic peaks was observed when the concentration of the target was increased from 5 fM to 50 nM. The formation of double-stranded DNA UCNPs (dsDNA-UCNPs) prevented their adsorption onto the GO surface and their fluorescence was retained. Fig. 3B shows the maximum intensity recorded for the two characteristic UCNP peaks at 540 nm and 655 nm as a function of cDNA concentration. It was observed
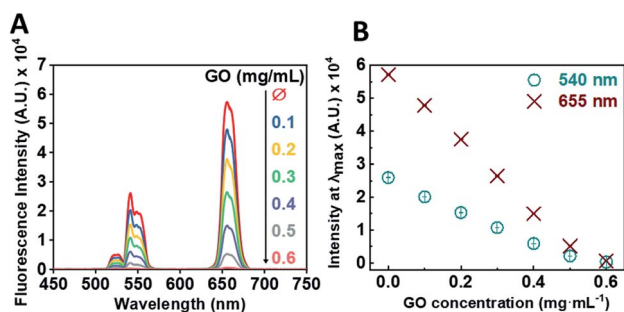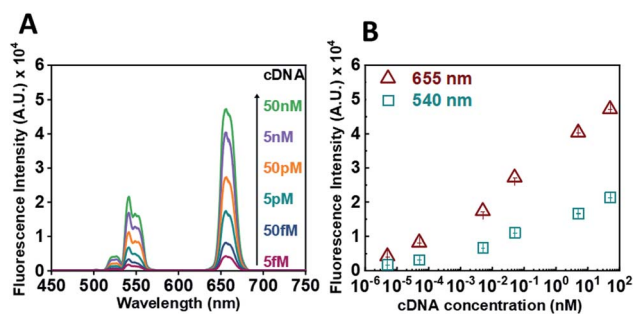
Fig. 3 (A) Representative fluorescence spectrum of oligonucleotide coated UNCPs (0.5 mg mL^{-1}) after incubation with increasing concentrations of cDNA targets in the presence of GO (B) graph of the maximum UCNP fluorescence intensity measured at 540 nm (cyan points) and 655 nm (red points) in the presence of GO as a function of cDNA concentration.

that at lower concentrations of cDNA the fluorescence intensity was weak. Most likely, this was due to a low number of duplexes present on the UCNPs which did not prevent some particles to adsorb to the GO surface. As the target concentration increased, the number of DNA duplexes on the nanoparticles also increased preventing the adsorption of nanoparticles to the GO surface and giving a strong fluorescent signal coming from the UCNPs. We further investigated the functionality of our sensor within biological fluids (see Fig. S5†) or by the use of a complementary RNA (cRNA) target (see Fig. S6†) as opposed to a cDNA target. In both instances our sensor demonstrated a rapid response to the complementary target.

The specificity of the sensor was further investigated to determine whether accurate detection could be ensured. Fig. 4 shows that upon incubation with a non-complementary DNA (ncDNA) target followed by the addition of GO (0.6 mg mL^{-1}) no fluorescence signal could be detected. As the concentration of the non-complementary target was progressively increased from 5 nM to 1000 nM the fluorescence signal remained quenched. This indicated that no duplex formation took place thus
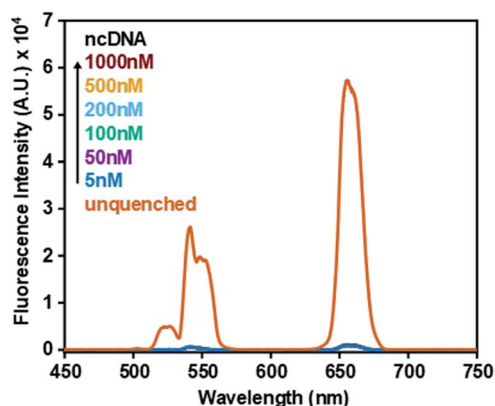
Fig. 2 (A) Representative fluorescence emission spectrum from oligonucleotide coated UCNPs (0.5 mg mL^{-1}) in the presence of increasing concentrations of GO. (B) Correlated fluorescence emission spectrum from oligonucleotide coated UCNPs (0.5 mg mL^{-1}) showing the decreasing fluorescence emission of the λ_{max} of the two typical peaks of UCNPs (655 nm, red points; 540 nm, cyan points) in the presence of increasing concentration of GO.

Fig. 4 Fluorescence spectrum of oligonucleotide coated UCNPs (0.5 mg mL^{-1}) in the absence of ncDNA and GO (unquenched) and in the presence of increasing concentrations of a ncDNA sequence and GO (0.6 mg mL^{-1}). For comparison the fluorescence spectrum of oligonucleotide coated UCNPs in the absence of GO is shown.

allowing ssDNA-UCNPs to adsorb to the GO surface leading to fluorescence quenching.

The lowest detected concentration in our experiments was 5 fM. This concentration was measured in bulk solution without concentration enrichment. The optical pumping was done using a focused pencil beam of around $20 \times 20 \times 500 \ \mu m^3$ dimensions, which excited UCNPs in a volume of 0.2 nL. At the concentration of 5 fM we therefore estimate a total number of 0.6 target copies in the detection volume at any given time. Furthermore, implementations might benefit from schemes in which further concentration of analytes is achieved through enrichment, ideally combined with a simple lateral flow configuration.[9,24,25]

In conclusion, we have demonstrated the construction of a sensor for the detection of a viral oligonucleotide target, a fingerprint of the SARS-CoV-2 virus with high sensitivity and specificity.

Conflicts of interest

There are no conflicts to declare.

Acknowledgements

Notes and references

1 J. F. Huggett, J. Moran-Gilad and J. E. Lee, COVID-19 new diagnostics development: novel detection methods for SARS-CoV-2 infection and considerations for their translation to routine use, *Curr. Opin. Pulm. Med.*, 2021, **27**(3), 155–162.

2 B. Singh, B. Datta, A. Ashish and G. Dutta, A comprehensive review on current COVID-19 detection methods: From lab care to point of care diagnosis, *Sensors International*, 2021, **2**, 100119.

3 N. Bhalla, P. Jolly, N. Formisano and P. Estrela, Introduction to biosensors, *Essays Biochem.*, 2016, **60**(1), 1–8.

4 P. Mehrotra, Biosensors and their applications – A review, *J. Oral Biol. Craniofacial Res.*, 2016, **6**(2), 153–159.

5 A. Mobed and E. Sepehri Shafigh, Biosensors promising bio-device for pandemic screening "COVID-19", *Microchem. J.*, 2021, **164**, 106094.

6 G. Seo, G. Lee, M. J. Kim, S.-H. Baek, M. Choi, K. B. Ku, C.-S. Lee, S. Jun, D. Park, H. G. Kim, S.-J. Kim, J.-O. Lee, B. T. Kim, E. C. Park and S. I. Kim, Rapid Detection of COVID-19 Causative Virus (SARS-CoV-2) in Human Nasopharyngeal Swab Specimens Using Field-Effect Transistor-Based Biosensor, *ACS Nano*, 2020, **14**(4), 5135–5142.

7 Z. Chen, Z. Zhang, X. Zhai, Y. Li, L. Lin, H. Zhao, L. Bian, P. Li, L. Yu, Y. Wu and G. Lin, Rapid and Sensitive Detection of anti-SARS-CoV-2 IgG, Using Lanthanide-Doped Nanoparticles-Based Lateral Flow Immunoassay, *Anal. Chem.*, 2020, **92**(10), 7226–7231.

8 P. Moitra, M. Alafeef, K. Dighe, M. B. Frieman and D. Pan, Selective Naked-Eye Detection of SARS-CoV-2 Mediated by N Gene Targeted Antisense Oligonucleotide Capped Plasmonic Nanoparticles, *ACS Nano*, 2020, **14**(6), 7617–7627.

9 D. Wang, S. He, X. Wang, Y. Yan, J. Liu, S. Wu, S. Liu, Y. Lei, M. Chen, L. Li, J. Zhang, L. Zhang, X. Hu, X. Zheng, J. Bai, Y. Zhang, Y. Zhang, M. Song and Y. Tang, Rapid lateral flow immunoassay for the fluorescence detection of SARS-CoV-2 RNA, *Nat. Biomed. Eng.*, 2020, **4**(12), 1150–1158.

10 M. Wang, G. Abbineni, A. Clevenger, C. Mao and S. Xu, Upconversion nanoparticles: synthesis, surface modification and biological applications, *Nanomed. Nanotechnol. Biol. Med.*, 2011, **7**(6), 710–729.

11 D. Mendez-Gonzalez, O. G. Calderón, S. Melle, J. González-Izquierdo, L. Bañares, D. López-Díaz, M. M. Velázquez, E. López-Cabarcos, J. Rubio-Retama and M. Laurenti, Contribution of resonance energy transfer to the luminescence quenching of upconversion nanoparticles with graphene oxide, *J. Colloid Interface Sci.*, 2020, **575**, 119–129.

12 Y. Li, Y. Li, D. Zhang, W. Tan, J. Shi, Z. Li, H. Liu, Y. Yu, L. Yang, X. Wang, Y. Gong and X. Zou, A fluorescence resonance energy transfer probe based on functionalized graphene oxide and upconversion nanoparticles for sensitive and rapid detection of zearalenone, *LWT*, 2021, **147**, 111541.

13 S. J. Wu, N. Duan, X. Y. Ma, Y. Xia, H. G. Wang, Z. P. Wang and Q. Zhang, Multiplexed Fluorescence Resonance Energy Transfer Aptasensor between Upconversion Nanoparticles and Graphene Oxide for the Simultaneous Determination of Mycotoxins, *Anal. Chem.*, 2012, **84**(14), 6263–6270.

14 Y. Rong, H. Li, Q. Ouyang, S. Ali and Q. Chen, Rapid and sensitive detection of diazinon in food based on the FRET between rare-earth doped upconversion nanoparticles and graphene oxide, *Spectrochim. Acta, Part A*, 2020, **239**, 118500.

15 M. S. Arai and A. S. S. de Camargo, Exploring the use of upconversion nanoparticles in chemical and biological sensors: from surface modifications to point-of-care devices, *Nanoscale Adv.*, 2021, **3**(18), 5135–5165.

16 P. Alonso-Cristobal, P. Vilela, A. El-Sagheer, E. Lopez-Cabarcos, T. Brown, O. L. Muskens, J. Rubio-Retama and A. G. Kanaras, Highly Sensitive DNA Sensor Based on Upconversion Nanoparticles and Graphene Oxide, *ACS Appl. Mater. Interfaces*, 2015, **7**(23), 12422–12429.

17 P. Vilela, A. El-Sagheer, T. M. Millar, T. Brown, O. L. Muskens and A. G. Kanaras, Graphene Oxide-Upconversion Nanoparticle Based Optical Sensors for Targeted Detection of mRNA Biomarkers Present in Alzheimer's Disease and Prostate Cancer, *ACS Sens.*, 2017, **2**(1), 52–56.

18 D. Giust, M. I. Lucio, A. H. El-Sagheer, T. Brown, L. E. Williams, O. L. Muskens and A. G. Kanaras, Graphene Oxide-Upconversion Nanoparticle Based Portable Sensors for Assessing Nutritional Deficiencies in Crops, *ACS Nano*, 2018, **12**(6), 6273–6279.

19 J. F.-W. Chan, C. C.-Y. Yip, K. K.-W. To, T. H.-C. Tang, S. C.-Y. Wong, K.-H. Leung, A. Y.-F. Fung, A. C.-K. Ng, Z. Zou, H.-W. Tsoi, G. K.-Y. Choi, A. R. Tam, V. C.-C. Cheng, K.-H. Chan, O. T.-Y. Tsang, K.-Y. Yuen and A. J. McAdam, Improved Molecular Diagnosis of COVID-19 by the Novel, Highly Sensitive and Specific COVID-19-RdRp/Hel Real-Time Reverse Transcription-PCR Assay Validated *In Vitro* and with Clinical Specimens, *J. Clin. Microbiol.*, 2020, **58**(5), e00310–e00320.

20 K. Alexaki, D. Giust, M. E. Kyriazi, A. H. El-Sagheer, T. Brown, O. L. Muskens and A. G. Kanaras, A DNA sensor based on upconversion nanoparticles and two-dimensional dichalcogenide materials, *Front. Chem. Sci. Eng.*, 2021, **15**(4), 935–943.

21 C. Homann, L. Krukewitt, F. Frenzel, B. Grauel, C. Würth, U. Resch-Genger and M. Haase, NaYF4:Yb,Er/NaYF4 Core/Shell Nanocrystals with High Upconversion Luminescence Quantum Yield, *Angew. Chem., Int. Ed.*, 2018, **57**(28), 8765–8769.

22 G. Yi, B. Sun, F. Yang, D. Chen, Y. Zhou and J. Cheng, Synthesis and Characterization of High-Efficiency Nanocrystal Up-Conversion Phosphors: Ytterbium and Erbium Codoped Lanthanum Molybdate, *Chem. Mater.*, 2002, **14**(7), 2910–2914.

23 Y. Jiang, W. Yin and H. E. Xu, RNA-dependent RNA polymerase: Structure, mechanism, and drug discovery for COVID-19, *Biochem. Biophys. Res. Commun.*, 2021, **538**, 47–53.

24 Y. Zhang, X. Liu, L. Wang, H. Yang, X. Zhang, C. Zhu, W. Wang, L. Yan and B. Li, Improvement in Detection Limit for Lateral Flow Assay of Biomacromolecules by Test-Zone Pre-enrichment, *Sci. Rep.*, 2020, **10**(1), 9604.

25 Y. Deng, H. Jiang, X. Li and X. Lv, Recent advances in sensitivity enhancement for lateral flow assay, *Mikrochim. Acta*, 2021, **188**(11), 379.